Carbohydrate Polymers 92 (2013) 1423–1431

Contents lists available at SciVerse ScienceDirect

Carbohydrate Polymers

journal homepage: www.elsevier.com/locate/carbpol

The photocrosslinkable tissue adhesive based on copolymeric dextran/HEMA

Tao Wang, Xueyan Mu, Haibo Li, Weilong Wu, Jun Nie, Dongzhi Yang*

Key Laboratory of Carbon Fiber and Functional Polymers, Ministry of Education, State Key Laboratory of Chemical Resource Engineering, Beijing University of Chemical Technology, Beijing 100029, China

ARTICLE INFO

Article history:
Received 30 July 2012
Received in revised form 27 August 2012
Accepted 24 September 2012
Available online 3 October 2012

Keywords:
Dextran
HEMA
Copolymerization
Tissue adhesive
Photocrosslinking

ABSTRACT

We developed a copolymeric bioadhesive system with the potential to be used as a tissue adhesive based on biopolymer dextran. Copolymeric hydrogels comprising a urethane dextran (Dex-U) and 2-hydroxyethyl methacrylate (HEMA) were prepared and crosslinked under the ultraviolet (UV) irradiation. In this study, the photopolymerization process was monitored by real time infrared spectroscopy (RTIR). The adhesion strength was evaluated by lap-shear-test. The surface tension, viscosity of the solutions and the cytotoxicity assays were investigated. Compared to Dex-U system, the addition of HEMA remarkably improved the properties of Dex-H system especially the adhesion strength and the nontoxicity. And materials variation could be tailored to match the need of tissues. The copolymeric tissue adhesives demonstrated promising adhesion strength and nontoxicity. The maximum adhesion strength reached to 4.33 ± 0.47 Mpa which was 86 times higher than that of Tisseel. The obtained products have the potential to serve as tissue adhesive in the future.

1. Introduction

Tissue adhesives were rapidly expanding its application in the field of medical areas. Tissue adhesives could often help tissue repair, reduce operative risk, promote would healing between disjoined tissues and introduce rapid hemostasis. Commercial biomedical adhesives could be classified into artificially synthetic and biological adhesives, such as the cyanoacrylate and fibrin. Cyanoacrylate adhesive was a compound synthesized by condensation of a cyanaocetate (Thumwanit & Kedjarune, 1999) with formaldehyde in the presence of a catalyst. It allowed rapid scar formation and would healing. Tremendous bonding strength and the ability to adhere to wet surfaces have expanded the use in medical area. But when polymerized in direct contact with the cell culture, cyanoacrylate caused excessive inflammation and tissue necrosis (Kim et al., 1995). Fibrin glue (Alston, Solen, Broderick, Sukavaneshvar, & Mohammad, 2007), associated with fibronectin, has been shown to improve the percentage of skin graft take, especially when associated with difficult grafting sites or sites associated with unavoidable movement. However, its bonding strength was relatively weak and its degradation was fast. So, it had predominantly been used to stop bleeding from parenchymatous organs such as the spleen or the liver. Problems with other tissue glues mostly arise from inadequate bonding strength in a watery milieu, which were the two most important issues when designing bone and tissue adhesives for use in the human body. Tradeoffs between various extremes of adhesion strength and biocompatibility were a major challenge.

Adhesives based on natural products like gelatin, collage, polysaccharide and biomimetic monomer L-3,4-dihydroxylphenylalanine (Lim, Kim, & Park, 2012) (DOPA) and its derivatives have been developed to overcome these disadvantages in commercial tissue adhesives.

Messersmith' groups (Brubaker, Kissler, Wang, Kaufman, & Messersmith, 2010; Brubaker & Messersmith, 2011; Fullenkamp et al., 2012; Lee et al., 2008; Lee, Messersmith, Israelachvili, & Waite, 2011) developed a series of mussel-inspired adhesives which obtained from branched water-soluble polyethylene glycol (PEG) polymers contained reactive catechol moieties to make use of the ability of the mussel to adhere to almost substrates in an aqueous environment. And with careful design of polymer composition and architecture, the adhesive ability could be improved. Polysaccharides, because of their inherently biomimetic physicochemical properties that allow for more interactions with proteins and cells, were attractive for applications of tissue adhesive. As reported (Bernkop-Schnürch, Kast, & Richter, 2001; Serrero et al., 2011; Serrero et al., 2010), after chemically modification, alginate, chitosan and starch could be used as adhesives in medical area.

Dextran was available and possessed a long history of both commercial and clinical use as plasma volume expanders (Dargan, 1962; Kolmonen et al., 2011), drug delivery carriers (Peng, Tomatsu, Korobko, & Kros, 2010), and wound cleansing and healing agents. Dextran (Nowakowska, Zapotoczny, Sterzel, & Kot, 2004) was a polymer of glucose in which the glucosidic linkages were

* Corresponding author. Tel.: +86 1064421310; fax: +86 1064421310.
E-mail address: yangdz@mail.buct.edu.cn (D. Yang).

0144-8617/$ – see front matter © 2012 Elsevier Ltd. All rights reserved.
http://dx.doi.org/10.1016/j.carbpol.2012.09.057

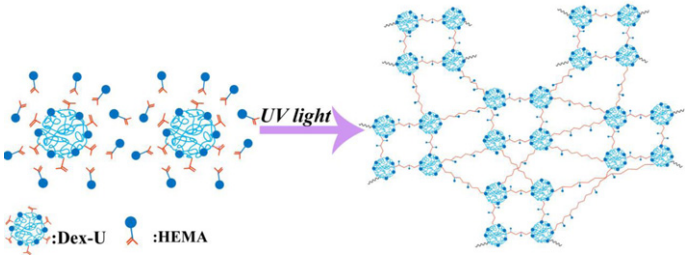

Scheme 1. Synthesis of Dex-U and gel networks formed by of Dex-H.

predominantly of the α-(1–6) type and its physical structure and properties have been well characterized (Ioan, Aberle, & Burchard, 2000a, 2000b, 2001). Structurally, there are abundant pendant hydroxyl groups in its anhydroglucose unit; dextran could be chemically modified to form hydrogels via cross-linking. Therefore, dextran effectively combined the advantages of synthetic and natural polymers as tissue adhesive and tissue engineering (Liu & Chan-Park, 2009; Liu & Chan-Park, 2010). Edelman (Artzi, Shazly, Baker, Bon, & Edelman, 2009; Artzi, Shazly, Crespo, et al., 2009; Artzi et al., 2011; Shazly, Artzi, Boehning, & Edelman, 2008; Shazly et al., 2010) created a family of copolymeric hydrogels featuring aminated star PEG and aldehyde dextran to meet the varying bioadhesive demands in the wide range of tissue composition and medical loading conditions. Sun (Sun & Chu, 2009; Sun et al., 2011) synthesized a series of functional dextran, including allyl isocyanate (Dex-AI), ethylamine (Dex-AE), chloroacetic acid (Dex-AC), or maleic-anhydride (Dex-AM). They integrated functional dextran and polyethylene glycol diacrylate (PEGDA) to get hybrid hydrogels for biomedical use. For several years, dextran hydrogels have been used in the field of tissue engineering (Lévesque & Shoichet, 2006; Yu & Shoichet, 2005) because of the non-cell-adhesive nature of dextran. Although dextran held good biocompatibility and biodegradability, inadequate mechanical properties and the long gelation time still are the issue for use of bioadhesive cannot be ignored.

In order to overcome the problem of a longer gel time, photocuring method was introduced. Recently photocuring process has been gained great attention in medical fields because the process of photoinitiating crosslinking is relatively simple, fast and mild. For in situ curing bioadhesives, these characteristics were the remarkably advantages. Since the adhesive gels could be prepared from liquids, they could be formed in situ following injection or similar in vitro invasive delivery. Furthermore, the gels could be controlled both temporally and spatially by altering monomer concentration, photoinitiator concentration, light intensity and exposure time to light source. For tissue adhesive, the non-cell-adhesive nature of dextran (Lévesque & Shoichet, 2006; Massia, Stark, & Letbetter, 2000) and delay of tissue healing were the problem that needs to be overcome.

2-Hydroxyethyl methacrylate (HEMA) was less harmful to the human body than any other reagents commonly used in photopolymerization biomaterials. Incorporating HEMA into polymer chains has garnered much attention, especially in the biomedical field. In the previous report, we have demonstrated a series of urethane methacrylated dextran derivatives used as bioadhesive which could completed crosslinking within 5 min and demonstrated good adhesion strength (Li, Niu, Yang, Nie, & Yang, 2011; Wang, Nie, & Yang, 2012). In this study, we aimed at designing a series of urethane methacrylated dextran based copolymeric bioadhesive by introducing HEMA (Scheme 1). We hoped that HEMA could not only increase the adhesion strength but also improve the cell adhesion. The properties of the adhesive system (called Dex-H) such as surface tension, adhesion strength, swelling ratio and photocrosslinking kinetics were measured. Cell adhesion and proliferation on hydrogels were also observed.

2. Experimental methods

2.1. Materials

Dextran (Mw 20 kDa) was purchased from Sinopharm Chemical Reagent Co. Ltd. (Shanghai, China) and 2-isocyanatoethyl methacrylate (IEMA) was purchased from Ginray Chemical Reagent Co. Ltd. (Shanghai, China), respectively. 2-Hydroxyethyl methacrylate (HEMA) and dibutyltion dilaurate (DBTL) as catalyst was purchased from Aladdin Reagent Co. (Shanghai, China). Photoinitiator 2-hydroxy-1-[4-(hydroxyethoxy) phenyl]-2-methyl-1-propanone (Darocur 2959) was supplied from Ciba-Geigy Chemical Co. (Tom River, NJ, USA). Dimethyl sulfoxide (extra dry DMSO, water <50 ppm) and other reagents were all obtained from Beijing Chemical Agent Co. (Beijing, China).

2.2. Preparation of urethane dextran derivatives (Dex-U)

The synthesis and characterization of the urethane methacrylated dextran (Dex-U) was published in our previously paper (Wang et al., 2012). Briefly, dextran reacted with 2-isocyanatoethyl methacrylate (IEMA) in the presence of DBTDL catalyst first. Eight grams of dextran, 0.05 g of DBTL were dissolved in 250 mL of DMSO after adding into a three-necked flack less than 40 °C and under nitrogen gas. Then, 7.5 g of IEMA dissolved in 80 mL DMSO was added dropwise within 3 h. Then the solution was poured into 800 mL of saturated sodium chloride solution with vigorous stirring. The white precipitate was filtrated and washed with distilled water for three times to remove DMSO and catalyst DBTL. Then the urethane methacrylated dextran was obtained after lyophilization. The different degrees of substitution (DS) of Dex-U could be got by adjusting molar ratio of IEMA to the hydroxyl groups of dextran. To improve the rate of gelation, the higher DS was desired, but when the DS > 0.5, the Dex-U could not dissolve in water. In order to obtain hydrogel system, we took the urethane dextran of DS 0.5. The determination of the structure of Dex-U was detected by FTIR and ^{1}H NMR (Li et al., 2011).

2.3. Preparation of dextran/HEMA (Dex-H) photocrosslinkable gels

Hydrogels were fabricated by photocrosslinking of precursor blend solutions (Dex-U and HEMA) which was called Dex-H. The 50 wt% precursor solutions were prepared with a range of solution with different weight ratio of Dex-U to HEMA as shown in Table 1. And the 1 wt% the photoinitiator Irgacure 2959 (D-2959) which had been proved to be the least cytotoxic to various cells was added above solution (Gao et al., 2010). The solution was injected into the cylindrical rubber mold after homogenizing. The system was irradiated under UV light source (320–480 nm, EXFOlite, EFOS Corporation, Mississauga, Canada) at the light intensity of UV light source was adjusted to 5, 10, 15, 30 and 50 mW/cm^2 to yield the photopolymerized hydrogels. The total solid content of the solutions about 40 and 60% was also discussed.

2.4. Surface tension and viscosity of different composition of Dex-H solutions

Surface tension of solutions was determined by an OCA20 video-based contact angle measuring device (Data-physics, Germany).

Viscosity measurements were made with an NDJ-1 rotation-viscometer. Viscosities of solutions with different weight ratio of Dex-U to HEMA at 50 wt% were detected.

Table 1
The compositions of photopolymerization Dex-H/HEMA hydrogel.

	Dex-H-1	Dex-H-2	Dex-H-3	Dex-H-4	Dex-H-5	Dex-H-6	Dex-H-7
Feed ratio[a]	10/0	8/2	6/4	5/5	4/6	2/8	0/10

[a] Feed ratio means the ratio of Dex-U to HEMA.

2.5. Measurement of photopolymerization kinetics of Dex-H

The double bond conversion of the gels was monitored by real-time near FTIR with the resolution of 4 cm^{-1} (Nicolet 5700, Thermo Electron, USA, equipped with an extended range KBr beam-splitter and an MCT/A detector). A horizontal transmission accessory (HTA) was designed to enable mounting of samples in a horizontal orientation for FTIR measurements. The change of C–H absorbance peak area (C–H, belong double bond) from 6110 to 6210 cm^{-1} in the near-IR range was correlated to the double bond conversion. For each sample, the series FTIR runs were repeated three times, and in most case, the error of double bond conversion was less than 2% (Zhou et al., 2008).

2.6. Measurement of adhesion strength

Spread uniformly on the surface, 30 wt% gelatin solutions was used to mimic the living tissue. The dimension of one piece of glass was 5 mm × 20 mm × 50 mm. After drying for 20 min at 70 °C, there was a homogenous sheet of gelatin on the surface of glass. Then, the pieces of glass were overlapped in 10 mm in which the Dex-H solution was spread and the area of bonding was 20 mm × 10 mm. They were irradiated by UV light under light intensity 30 mW/cm^2 for 5 min. The Dex-H was crosslinked between the gelatin sheets. The glass samples after UV curing were tested by using a universal testing machine (Model 1185, Instron, USA) with a crosshead speed of 5 mm/min at room temperature. For each experiment, five samples were measured and recorded the average of these values.

2.7. Measurement of swelling kinetics

The sol-removed dry gels (weight W_0) were immersed in PBS at 37 °C with constant shake. The swollen hydrogel disks were withdrawn on a filter paper after certain time intervals. After removal of the excess superficial water, the weight of the samples in the swollen state (W_s) was measured until swelling equilibrium was reached. Swelling ratio of hydrogel was calculated by the following equation (Kim, Won, & Chu, 1999):

$$\text{Swelling ratio}\,(\%) = \frac{W_s - W_0}{W_0} \times 100 \quad (1)$$

2.8. X-ray diffraction (XRD) study of gels

X-ray diffraction (XRD) patterns of the Dex-H gels were recorded on an X-ray diffractometer (D/Max 2500VB2+/Pc, Rigaku, Japan) with C_uK characteristic radiation (wavelength 0.154 nm) at a voltage of 40 kV and a current of 50 mA. The scanning rate was 10°/min and the scanning scope was at 5–90° at room temperature.

2.9. Scanning electron microscopy (SEM)

The surface and internal morphology of cross-linked Dex-H gels were examined by SEM. Lyophilized gels were fractured after cooling in liquid nitrogen to expose the structure inside the gels. Samples were mounted and sputter coated with gold/palladium by scanning electron microscopy (SEM; Hitachi, S-4700, Japan). In order to investigate the extent of self-polymerization of the HEMA, the surface and internal morphology of Dex-H gels which had been immersed in ethanol solvent for 24 h were also observed.

2.10. Cytotoxicity assays

The cytotoxicity of the gel samples was evaluated based on a procedure adapted from the ISO10993-5 standard test method. Mouse fibroblasts (L929) were cultured in DMEM medium supplemented with 10% fetal bovine serum, together with 1.0% penicillin–streptomycin, and 1.2% glutamine. Culture was maintained at 37 °C in a wet atmosphere containing 5% CO_2. When the cells reached 80% confluence, they were trypsinized with 0.25% trypsin containing 1×10^3 M ethylene diaminetetraacetic acid (EDTA).For viability testing, MTT (3-[4,-dimethylthiazol-2-yl]-2,5-diphenyltetrazolium bromide; Thiazolyl blue) assay were carried out. For the MTT assay, the samples with ~0.2 mm thickness were placed in wells of 24-well culture plate after being sterilized with highly compressed steam for 15 min. The samples were then incubated in 1 mL DMEM medium at 37 °C for 24 h and the extraction ratio is 100 mg/mL. In the end, the samples were removed, and it could obtain the so-called extracts. L929 cells were seeded in wells of 96-well plate at a density of 103 cells per well. When incubated for 24 h, the culture medium was removed and replaced with the as-prepared extraction medium and incubated for another 24 h, and then 100 μL MTT solution was added to each well. After 4 h incubation at 37 °C, 200 μL of DMSO was added to dissolve the formazan crystals. The dissolved solution was swirled homogeneously about 10 min by the shaker. The optical density (OD) of the formazan solution was measured by an ELISA reader (Multiscan MK3, Labsystem Co., Finland) at 570 nm. The relative cell viability was calculated by the following equation:

$$\text{relative cell viability}\,(\%) = \frac{OD_{treated}}{OD_{control}} \times 100 \quad (2)$$

where $OD_{control}$ was obtained in the absence of samples, and $OD_{treated}$ was obtained in the presence of samples.

After 48 h of culturing of the prepared circular samples, cellular constructs were harvested, rinsed with PBS to remove non-adherent cells. Subsequently, fixed them with 3.0% glutaraldehyde at 4 °C for 4 h. After that the samples were dehydrated through a series of graded ethanol solutions and air-dried overnight. Dry samples were sputtered with gold for observation of cell morphology on the surface of the scaffolds by scanning electron microscope (Hitachi, S-4700, Japan).

3. Results and discussion

3.1. Surface tension analysis

For adhesives, one of the most important parameters was surface tension of adhesive. The dispersion of adherend and steady performance after crosslinking were all affected by the surface tension. The surface tension of adhesive solution must be equal to or less than the one of adherend. The surface energy of skin varied from 38 to 56 mN/m under different relative humidity and temperature.(Venkatraman & Gale, 1998). The surface

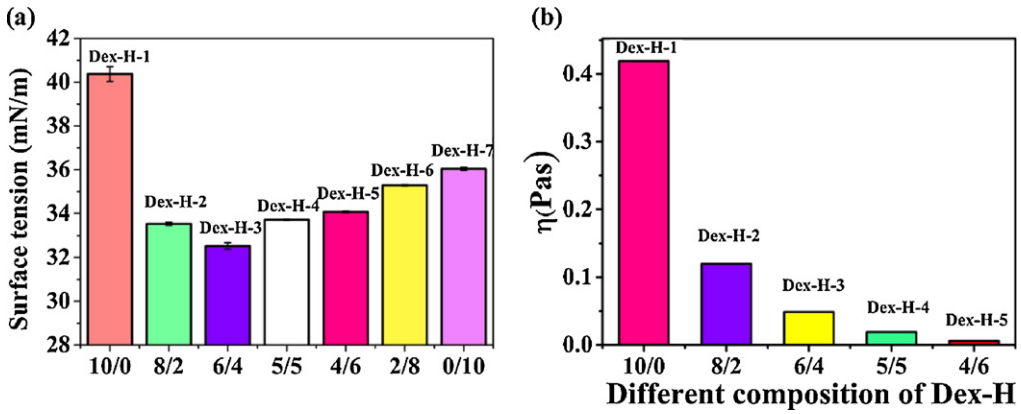

Fig. 1. Surface tension (a) and viscosity (b) of different composition of Dex-H solution.

tension of blood was 47.5 mN/m by the sessile drop method at 37 °C (Agathopoulos & Nikolopoulos, 1995).

Surface tension of different composition of Dex-H solution is shown in Fig. 1(a). It firstly decreased and then increased with increase of HEMA, and Dex-H-3 reached the minimum 32.5 ± 0.15 mN/m. Mother nature drove all system to a minimum energy state, so in order to minimize surface energy, polar groups orient away from the surface in air or toward the more polar phase at aqueous interfaces. After the addition of hydrophilic HEMA, non-polar groups ($-C_mH_{2m+1}$) were exposed to the air to minimize surface energy while polar groups (—OH) were exposed in the water to minimize the interfacial energy of the Dex-H solutions. When the addition of HEMA reached to a threshold, the molecular composition of surface showed no further change so as to obtain the minimal surface tension for Dex-H-3 at 32.5 ± 0.15 mN/m. The surface tension of the solution was less than or close to the scope of the surface tension of human skin that would help the solutions to spread easily on the skin to confirm the adhesiveness.

As shown in Fig. 1(b), the value of viscosity of different composition of Dex-H solutions decreased to 0.006 Pa s with the decrease of the content of Dex-U. And when the weight ratio of Dex-U to HEMA decreased to 2/8, the actual viscosity of solutions was too low to be measured.

Dex-U was a kind of polyfunctional macromolecules which behaved as entangled random coil chain in aqueous solution. The more macromolecules, the more serious it entangled that leading to the increase of the viscosity. On one side, the addition of the low viscosity HEMA replaced the entangled Dex-U to decrease the viscosity of the system. On the other side, the —OH groups in HEMA can form hydrogen bond with —OH groups of Dex-U in water. Coated with a layer of small molecule, the entanglement would be broken. So the addition of HEMA decreased the viscosity of the solutions.

3.2. Photocrosslinking kinetics of Dex-H

When the Dex-H solution was crosslinked by UV irradiation, the unsaturated C=C double bonds of Dex-U started polymerize and the area of absorption peak attributed to C=C double bond of methacrylate at 6120–6210 cm^{-1} decreased accordingly. The influence of the weight ratio of Dex-U to HEMA on photocrosslinking process is shown in Fig. 2(a), and it could be observed that the conversion rate and the eventual conversion of the gels contained Dex-U were obviously greater than neat HEMA gels. If there was Dex-U, the eventual conversion could reach to 100%. But the conversion rate decreased with the increase of the content of HEMA. The eventual conversion of double bonds of HEMA solution could only reached 20% which could not form stable solid gel after exposing to UV light for 5 min. The increase of the content of polyfunctional Dex-U increased the viscosity of solution which could hinder the termination of free radical and easily produce an auto-acceleration. The more of Dex-U led to the faster the conversion rate and the higher the eventual conversion. The effect of the total solid content was also demonstrated in Fig. 2(b). The higher total solid content correspond to the higher viscosity and therefore led to the higher the conversion rate and the eventual conversion.

The influence of initiator D-2959 was performed in Fig. 2(c). When increasing the content of D-2959 from 0.1% to 3%, both the max conversion rate and the eventual conversion of methacrylate double bonds were improved, which resulted from the more free radicals released by D-2959. But when further increasing the content of the photoinitiator, the max conversion rate and eventual conversion tended to be constant. This might be the result of light shielding effect, which was induced by combination termination of excessive free radicals produced by D-2959. Fig. 2(d) shows the influence of UV light intensity from 10 mW/cm^2 to 50 mW/cm^2. The higher the UV light intensity, the more free radicals produced by photoinitiator D-2959 which resulted to increase of the max conversion rate and eventual conversion of methacrylate double bonds. Considered the balance of low cell injury and high polymerization rate by high light intensity, light intensity of 30 mW/cm^2 was selected.

3.3. Evaluation of adhesion strength

Lap shear tests are commonly found in the literature to assess adhesive strength for bonding biological tissue (Burke, Ritter-Jones, Lee, & Messersmith, 2007). We used lap shear test to evaluate the adhesive performance of Dex-H gels. The samples for lap shear test were prepared by placing Dex-H gels between gelatin sheets to simulate the living tissues. The methods were adapted from ASTM F2255-03 “Standard Test Method for Strength Properties of Tissue Adhesive in Lap-Shear by Tension Loading”.

Adhesion strength of different composition of Dex-H solution is shown in Fig. 3(b). The adhesion strength was improved from 1.69 ± 0.14 Mpa to 4.33 ± 0.47 Mpa with the weight ratio of Dex-U to HEMA decreased from 10/0 to 6/4. Polyfunctional Dex-U that was considered as crosslinker provided sufficient cohesion. Compared with Dex-U, before polymerization, monofunctional small molecular HEMA was easy to penetrate into the surface groove of gelatin to form mechanical interlocking. But when the weight ratio of Dex-H to HEMA decreased to 0/10, excessive HEMA decreased the crosslinking density so that the adhesion strength plummeted

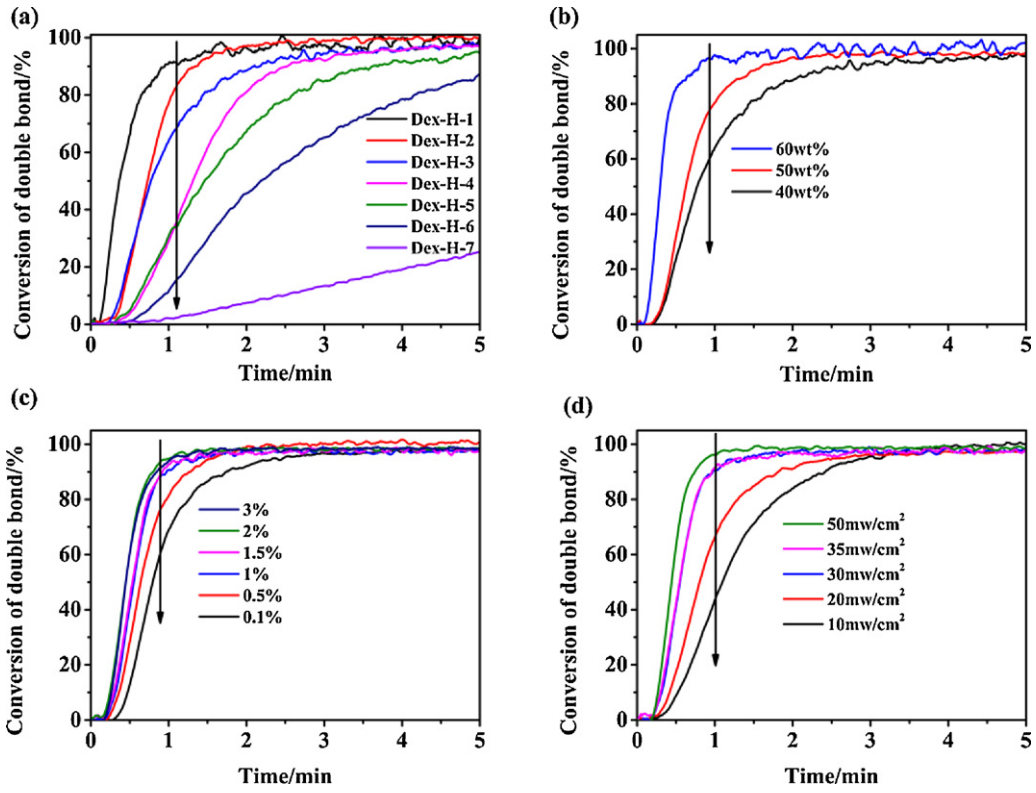

Fig. 2. Photopolymerization kinetics of Dex-H in different composition (a), different total solid content (b), different content of initiator (c) and different light intensity (d).

to 1.36 ± 0.29 Mpa. Insufficient cohesion caused the decrease of adhesion. In Fig. 3(c), the increase of the total solid content reduced the adhesion strength slightly. Too much cohesion brought down the interfacial adhesion.

The adhesive properties of the Dex-H gels were compared to commercial available bioadhesives Tisseel (a fibrin adhesive). The Dex-H-3 gel exhibited the highest adhesion strength. For example, Dex-H-3 gel (4.33 ± 0.47 Mpa) which were 86 times higher than that of Tisseel (0.05 MPa) (Alston et al., 2007).

3.4. Measurement of swelling kinetics

When polymer was used in the field of biomaterials, swelling ratio was one of the important indicators to evaluate the adhesive performance. High swelling ratio formed compression in the vessel tissue of implantation even in hard tissue. This phenomenon hindered the recovery process and caused infections.

Fig. 4 shows the swelling kinetics of Dex-H gels, when incubated in PBS at pH 7.4. The swelling ratio increased with the

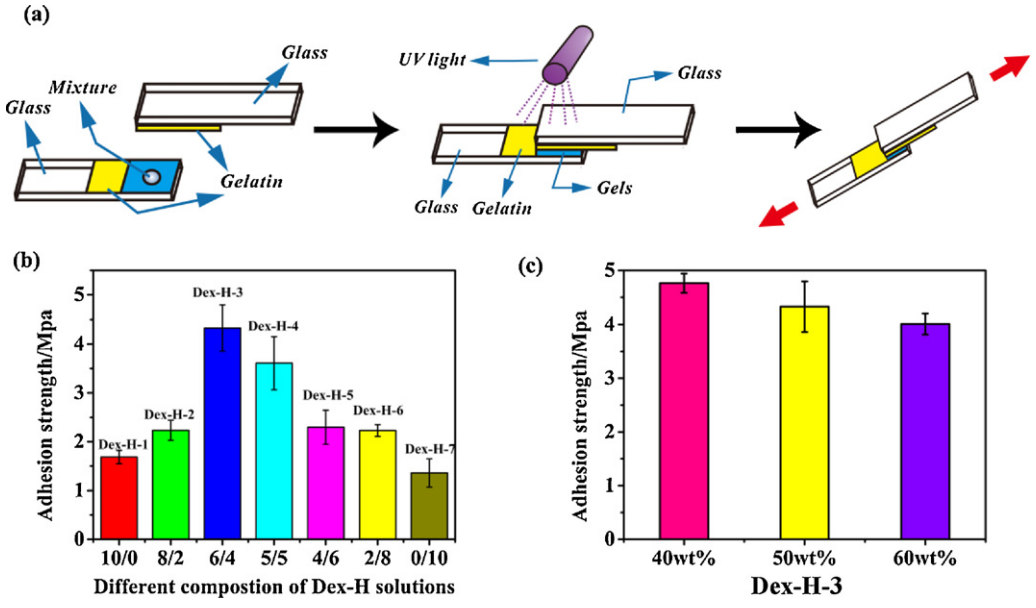

Fig. 3. (a) The schematic of preparation of lap-shear sample; adhesion strength of Dex-H solution of different composition (b) and different total solid content (c).

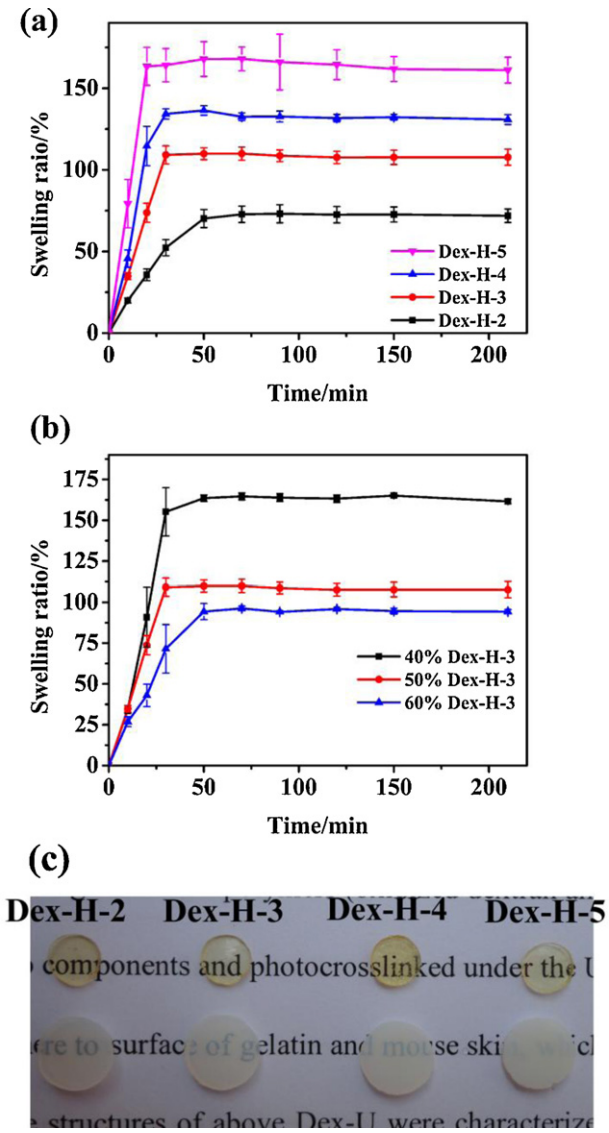

Fig. 4. Swelling kinetics of hydrogels of Dex-H of different composition (a), different total solid content of Dex-H-3 gels (b) and the before and after swelling photo of Dex-H gels (c).

promotion of the content of HEMA. The addition of HEMA decreased the crosslinking density so that led to the increase of swelling ratio as presented in Fig. 4(a). The swelling ratio 72% of Dex-H-2 increased to 167% of Dex-H-5. While in Fig. 4(b), the higher total solid content of gels possessed higher crosslinking density which could control the swelling ratio. Therefore, we must strike a balance between the total solid content and the proportion of HEMA in order to get optimal swelling ratio.

3.5. X-ray diffraction (XRD) study of gels

Fig. 5 presents the XRD patterns of Dex-H-1, Dex-H-4 and Dex-H-7 gels after natural drying. It could be seen that Dex-H-7 gels exhibited three typical peaks at $2\theta = 18.84^\circ$, 30.84° and 41.12°, agreed to Jie Song's observation that *p*(HEMA) possessed three typical peaks (Song, Saiz, & Bertozzi, 2003). The XRD patterns of Dex-H gels changed with the variation of the weight ration of Dex-U to HEMA. Amorphous Dex-U hindered the formation of inter- and intra-molecular hydrogen bonds thus forming a

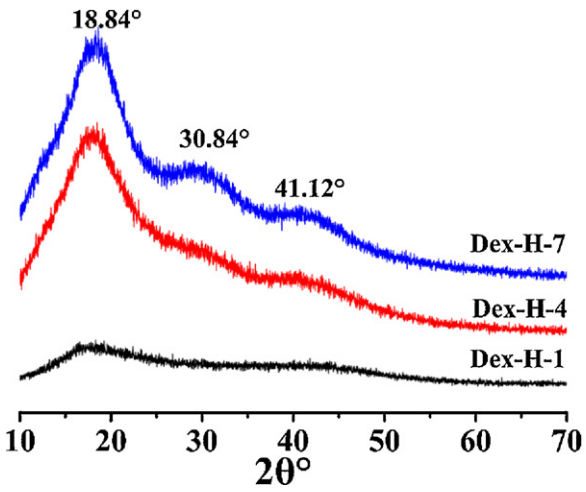

Fig. 5. XRD patterns of Dex-H gels of different composition.

small fraction of crystalline phase and a larger fraction of amorphous phase. Dex-H-4 had one peak at around $2\theta = 18.84^\circ$ and it also presented weak crystallinity. XRD patterns also indicated that Dex-U and HEMA formed good interpenetrating copolymeric networks.

3.6. Scanning electron microscopy (SEM)

The surface and interior morphology of Dex-H gels after lyophilization were demonstrated in Fig. 6(a)–(d). Compared to Dex-H-1, the surface of Dex-H-3 was smooth and uniform and there were light areas in the fracture surface. Under the high magnification in Fig. 6(d), the difference between light and dark might be caused by contrast. The copolymeric chain segment possessed different electron intensity in comparison to the general chain segment so as to cause the contrast.

Fig. 6(e)–(j) demonstrats the surface and internal morphology of the ethanol solvent treated Dex-H gels for that *p*(HEMA) could be dissolved in ethanol. With the increase of the content of HEMA from the Dex-H-3 gels to the Dex-H-5 gels, the marks that *p*(HEMA) had been wash away became more and more obviously. While in the facture surfaces in Fig. 6(f), (h), and (j), it could be found that there were no obvious marks as in the surfaces. This could indirect prove that the addition of monofunctional small molecular HEMA inclined to spread to the surface of the solutions.

3.7. Cytotoxicity assays

Fig. 7(a) shows the selected SEM images of mouse fibro-blast L929 cell seeded on the surface of the Dex-H-1 and Dex-H-3 hydrogels after 48 h culture. The L929 cells spread quite well on the surface of all hydrogels indicating good cell-surface interaction and good cell viability on the Dex-H-3 gels surface as shown in Fig. 7(a2) and (a3). While in Fig. 7(a1), cells could not spread well on the surface of Dex-H-1. The addition of HEMA helped improve the cell attachment on the surface of the Dex-H hydrogels.

An ideal bioadhesive should not release toxic products or produce adverse reactions that can be evaluated through in vitro cytotoxic tests. It is a basic property for a biomaterial. Fig. 7b demonstrates the absorbance obtained from a MTT assay of L929 cells which were cultured with the extraction media from various types of specimens. It could be seen from Fig. 7c, the average viability of the cell still reached above 90% of that of the negative control at 72 h and no statistically significant differences ($p > 0.05$) were

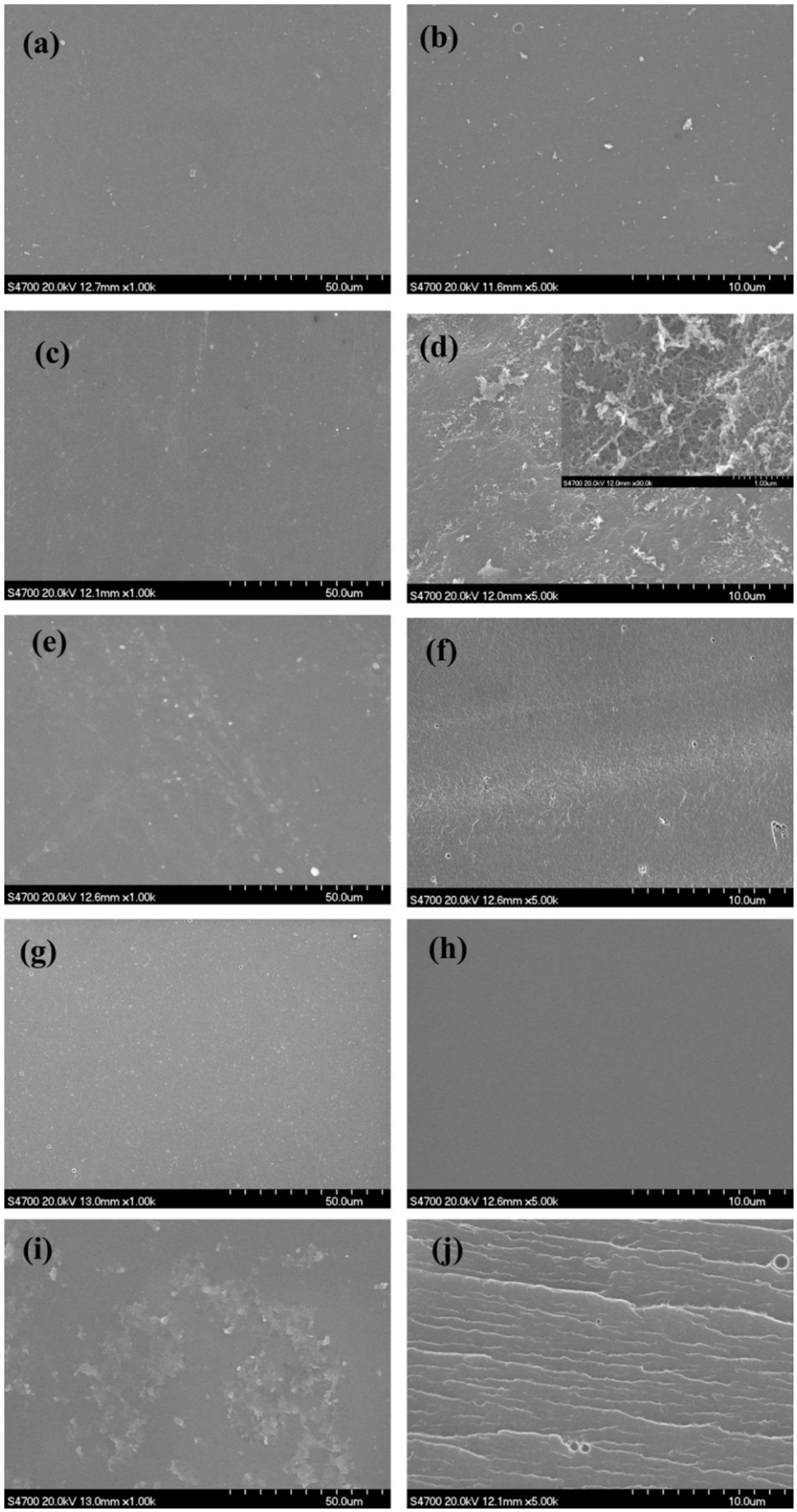

Fig. 6. SEM images of Dex-H hydrogels with different composition after lyophilization: surface (a) and fracture surface (b) of Dex-H-1; surface (c) and fracture surface (d) of Dex-H-3; solvent treated surface (e), (g), and (i) and fracture surface (f), (h), and (j) of Dex-H-3, Dex-H-4 and Dex-H-5, respectively.

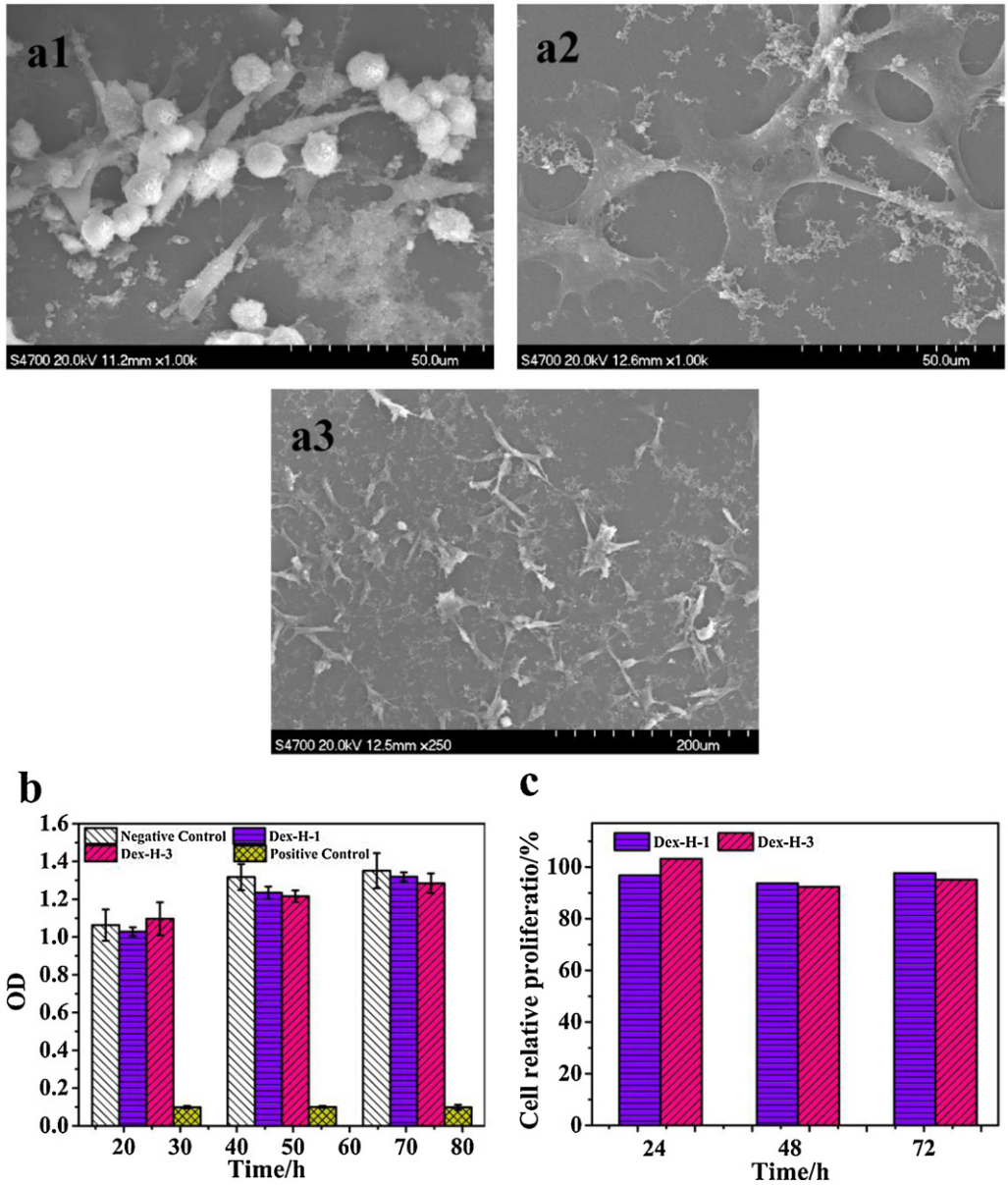

Fig. 7. Fluorescence microscopy images and selected SEM images of L929 cell seeded on the surface of the Dex-H-1 (a1) and Dex-H-3 (a2 and a3); (b) MTT test of Dex-H hydrogels with positive and negative controls, $^{*}p > 0.05$ predicated not statistically significant differences when compared to the negative control of indirect cytotoxicity. The data represented mean and standard deviations of six samples; (c) cell relative proliferation.

observed in the cell activity within 72 h in the presence of the most of the hydrogels extracts in comparison with negative control. This indicated that the Dex-H gels were less toxic to L929 cells.

4. Conclusion

In this study, we prepared a photocrosslinkable copolymeric bioadhesive system (Dex-H system) by consisting of dextran derivatives (Dex-U) and HEMA. The incorporation of HEMA significantly promoted the properties of Dex-H adhesives that superior to Dex-U adhesives. The results of lap shear tests showed that the copolymerization of HEMA and Dex-U especially when the weight ratio of Dex-U to HEMA at 6/4 dramatically increased the adhesion strength to 4.33 ± 0.47 Mpa. It was about 86 times that of Tisseel.

But we still need to explore the approach to solve the problem of the excessive swelling ratio which might hinder the recovery process and caused infections.

Acknowledgements

The author would like to thank the National Natural Science Foundation of China (51273015) Beijing Natural Science Foundation 2112033 Study on the molecular design and properties of new photocurable antifouling coatings and the Fundamental Research Funds for the Central Universities ZZ1115 for its financial support.

References

Agathopoulos, S., & Nikolopoulos, P. (1995). Wettability and interfacial interactions in bioceramic–body–liquid systems. *Journal of Biomedical Materials Research*, *29*, 421–429.

Alston, S. M., Solen, K. A., Broderick, A. H., Sukavaneshvar, S., & Mohammad, S. F. (2007). New method to prepare autologous fibrin glue on demand. *Translational Research*, *149*, 187–195.

Artzi, N., Shazly, T., Baker, A. B., Bon, A., & Edelman, E. R. (2009). Aldehyde–amine chemistry enables modulated biosealants with tissue-specific adhesion. *Advanced Materials*, *21*, 3399–3403.

Artzi, N., Shazly, T., Crespo, C., Ramos, A. B., Chenault, H. K., & Edelman, E. R. (2009). Characterization of star adhesive sealants based on PEG/dextran hydrogels. *Macromolecular Bioscience*, *9*, 754–765.

Artzi, N., Zeiger, A., Boehning, F., bon Ramos, A., Van Vliet, K., & Edelman, E. R. (2011). Tuning adhesion failure strength for tissue-specific applications. *Acta Biomaterialia*, *7*, 67–74.

Bernkop-Schnürch, A., Kast, C. E., & Richter, M. F. (2001). Improvement in the mucoadhesive properties of alginate by the covalent attachment of cysteine. *Journal of Controlled Release*, *71*, 277–285.

Brubaker, C. E., Kissler, H., Wang, L.-J., Kaufman, D. B., & Messersmith, P. B. (2010). Biological performance of mussel-inspired adhesive in extrahepatic islet transplantation. *Biomaterials*, *31*, 420–427.

Brubaker, C. E., & Messersmith, P. B. (2011). Enzymatically degradable mussel-inspired adhesive hydrogel. *Biomacromolecules*, *12*, 4326–4334.

Burke, S. A., Ritter-Jones, M., Lee, B. P., & Messersmith, P. B. (2007). Thermal gelation and tissue adhesion of biomimetic hydrogels. *Biomedical Materials*, *2*, 203.

Dargan El, M. W. H. E. J. O. A. (1962). CLinical evaluation of a new dextran plasma expander. *JAMA: The Journal of the American Medical Association*, *179*, 203–206.

Fullenkamp, D. E., Rivera, J. G., Gong, Y.-k., Lau, K. H. A., He, L., Varshney, R., et al. (2012). Mussel-inspired silver-releasing antibacterial hydrogels. *Biomaterials*, *33*, 3783–3791.

Gao, X., Zhou, Y., Ma, G., Shi, S., Yang, D., Lu, F., et al. (2010). A water-soluble photocrosslinkable chitosan derivative prepared by Michael-addition reaction as a precursor for injectable hydrogel. *Carbohydrate Polymers*, *79*, 507–512.

Ioan, C. E., Aberle, T., & Burchard, W. (2000a). Light scattering and viscosity behavior of dextran in semidilute solution. *Macromolecules*, *34*, 326–336.

Ioan, C. E., Aberle, T., & Burchard, W. (2000b). Structure Properties of Dextran. 2. Dilute Solution. *Macromolecules*, *33*, 5730–5739.

Ioan, C. E., Aberle, T., & Burchard, W. (2001). Structure properties of dextran. 3. Shrinking factors of individual clusters. *Macromolecules*, *34*, 3765–3771.

Kim, J. C., Bassage, S. D., Kempski, M. H., del Cerro, M., Park, S. B., & Aquavella, J. V. (1995). Evaluation of tissue adhesives in closure of scleral tunnel incisions. *Journal of Cataract and Refractive Surgery*, *21*, 320–325.

Kim, S. H., Won, C. Y., & Chu, C. C. (1999). Synthesis and characterization of dextran-based hydrogel prepared by photocrosslinking. *Carbohydrate Polymers*, *40*, 183–190.

Kolmonen, M., Leinonen, A., Kuuranne, T., Pelander, A., Deventer, K., & Ojanperä, I. (2011). Specific screening method for dextran and hydroxyethyl starch in human urine by size exclusion chromatography-in-source collision-induced dissociation-time-of-flight mass spectrometry. *Analytical and Bioanalytical Chemistry*, *401*, 563–571.

Lee, B. P., Messersmith, P. B., Israelachvili, J. N., & Waite, J. H. (2011). Mussel-inspired adhesives and coatings. *Annual Review of Materials Research*, *41*, 99–132.

Lee, H., Lee, Y., Statz, A. R., Rho, J., Park, T. G., & Messersmith, P. B. (2008). Substrate-independent layer-by-layer assembly by using mussel-adhesive-inspired polymers. *Advanced Materials*, *20*, 1619–1623.

Lévesque, S. G., & Shoichet, M. S. (2006). Synthesis of cell-adhesive dextran hydrogels and macroporous scaffolds. *Biomaterials*, *27*, 5277–5285.

Li, H., Niu, R., Yang, J., Nie, J., & Yang, D. (2011). Photocrosslinkable tissue adhesive based on dextran. *Carbohydrate Polymers*, *86*, 1578–1585.

Lim, J. I., Kim, J. H., & Park, H.-K. (2012). The adhesive properties of prepolymerized allyl 2-cyanoacrylate/poly L-3,4-dihydroxyphenylalanine for use as bioglue. *Materials Letters*, *81*, 251–253.

Liu, Y., & Chan-Park, M. B. (2009). Hydrogel based on interpenetrating polymer networks of dextran and gelatin for vascular tissue engineering. *Biomaterials*, *30*, 196–207.

Liu, Y., & Chan-Park, M. B. (2010). A biomimetic hydrogel based on methacrylated dextran-graft-lysine and gelatin for 3D smooth muscle cell culture. *Biomaterials*, *31*, 1158–1170.

Massia, S. P., Stark, J., & Letbetter, D. S. (2000). Surface-immobilized dextran limits cell adhesion and spreading. *Biomaterials*, *21*, 2253–2261.

Nowakowska, M., Zapotoczny, S., Sterzel, M., & Kot, E. (2004). Novel water-soluble photosensitizers from dextrans. *Biomacromolecules*, *5*, 1009–1014.

Peng, K., Tomatsu, I., Korobko, A. V., & Kros, A. (2010). Cyclodextrin–dextran based in situ hydrogel formation: A carrier for hydrophobic drugs. *Soft Matter*, *6*, 85–87.

Serrero, A. l., Trombotto, S. p., Bayon, Y., Gravagna, P., Montanari, S., & David, L. (2011). Polysaccharide-based adhesive for biomedical applications: Correlation between rheological behavior and adhesion. *Biomacromolecules*, *12*, 1556–1566.

Serrero, A. l., Trombotto, S. p., Cassagnau, P., Bayon, Y., Gravagna, P., Montanari, S., et al. (2010). Polysaccharide gels based on chitosan and modified starch: Structural characterization and linear viscoelastic behavior. *Biomacromolecules*, *11*, 1534–1543.

Shazly, T. M., Artzi, N., Boehning, F., & Edelman, E. R. (2008). Viscoelastic adhesive mechanics of aldehyde-mediated soft tissue sealants. *Biomaterials*, *29*, 4584–4591.

Shazly, T. M., Baker, A. B., Naber, J. R., Bon, A., Van Vliet, K. J., & Edelman, E. R. (2010). Augmentation of postswelling surgical sealant potential of adhesive hydrogels. *Journal of Biomedical Materials Research Part A*, *95*, 1159–1169.

Song, J., Saiz, E., & Bertozzi, C. R. (2003). Preparation of pHEMA–CP composites with high interfacial adhesion via template-driven mineralization. *Journal of the European Ceramic Society*, *23*, 2905–2919.

Sun, G., & Chu, C.-C. (2009). Impregnation of tubular self-assemblies into dextran hydrogels. *Langmuir*, *26*, 2831–2838.

Sun, G., Shen, Y.-I., Kusuma, S., Fox-Talbot, K., Steenbergen, C. J., & Gerecht, S. (2011). Functional neovascularization of biodegradable dextran hydrogels with multiple angiogenic growth factors. *Biomaterials*, *32*, 95–106.

Thumwanit, V., & Kedjarune, U. (1999). Cytotoxicity of polymerized commercial cyanoacrylate adhesive on cultured human oral fibroblasts. *Australian Dental Journal*, *44*, 248–252.

Venkatraman, S., & Gale, R. (1998). Skin adhesives and skin adhesion. 1. Transdermal drug delivery systems. *Biomaterials*, *19*, 1119–1136.

Wang, T., Nie, J., & Yang, D. (2012). Dextran and gelatin based photocrosslinkable tissue adhesive. *Carbohydrate Polymers*, http://dx.doi.org/10.1016/j.carbpol.2012.07.011

Yu, T. T., & Shoichet, M. S. (2005). Guided cell adhesion and outgrowth in peptide-modified channels for neural tissue engineering. *Biomaterials*, *26*, 1507–1514.

Zhou, Y., Yang, D., Ma, G., Tan, H., Jin, Y., & Nie, J. (2008). A pH-sensitive water-soluble N-carboxyethyl chitosan/poly(hydroxyethyl methacrylate) hydrogel as a potential drug sustained release matrix prepared by photopolymerization technique. *Polymers for Advanced Technologies*, *19*, 1133–1141.